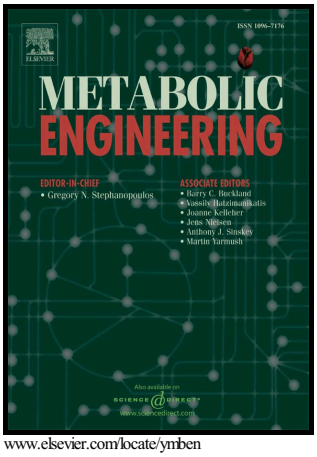

www.elsevier.com/locate/ymben

L-lysine production independent of the oxidative pentose phosphate pathway by *corynebacterium glutamicum* with the *streptococcus mutans gapN* gene

Seiki Takeno, Kazumasa Hori, Sachiko Ohtani, Akinori Mimura, Satoshi Mitsuhashi, Masato Ikeda

PII: S1096-7176(16)30007-6
DOI: http://dx.doi.org/10.1016/j.ymben.2016.03.007
Reference: YMBEN1107

To appear in: *Metabolic Engineering*

Received date: 30 November 2015
Revised date: 16 February 2016
Accepted date: 25 March 2016

Cite this article as: Seiki Takeno, Kazumasa Hori, Sachiko Ohtani, Akinor Mimura, Satoshi Mitsuhashi and Masato Ikeda, L-lysine production independer of the oxidative pentose phosphate pathway by *corynebacterium glutamicur* with the *streptococcus mutans gapN* gene, *Metabolic Engineering* http://dx.doi.org/10.1016/j.ymben.2016.03.007

L-Lysine production independent of the oxidative pentose phosphate pathway by *Corynebacterium glutamicum* with the *Streptococcus mutans gapN* gene

Seiki Takeno[a], Kazumasa Hori[a], Sachiko Ohtani[a], Akinori Mimura[a], Satoshi Mitsuhashi[b], Masato Ikeda[a,*]

[a]Department of Agricultural and Life Sciences, Faculty of Agriculture Shinshu University, Nagano 399-4598, Japan

[b]Bioprocess Development Center, Kyowa Hakko Bio Co., Ltd., Tsukuba, Ibaraki 305-0841, Japan

*Corresponding author: Masato Ikeda, Department of Agricultural and Life Sciences, Faculty of Agriculture, Shinshu University, Nagano 399-4598, Japan. Phone: +81-265-77-1614; Fax: +81-265-77-1629; E-mail: m_ikeda@shinshu-u.ac.jp

Abstract

We have recently developed a *Corynebacterium glutamicum* strain that generates NADPH via the glycolytic pathway by replacing endogenous NAD-dependent glyceraldehyde 3-phosphate dehydrogenase (GapA) with a nonphosphorylating NADP-dependent glyceraldehyde 3-phosphate dehydrogenase (GapN) from *Streptococcus mutans*. Strain RE2, a suppressor mutant spontaneously isolated for its improved growth on glucose from the engineered strain, was proven to be a high-potential host for L-lysine production (Takeno et al., 2010). In this study, the suppressor mutation was identified to be a point mutation in *rho* encoding the transcription termination factor Rho. Strain RE2 still showed retarded growth despite the mutation *rho696*. Our strategy for reconciling improved growth with a high level of L-lysine production was to use GapA together with GapN only in the early growth phase, and subsequently shift this combination-type glycolysis to one that depends only on GapN in the rest of the growth phase. To achieve this, we expressed *gapA* under the

myo-inositol-inducible promoter of *iolT1* encoding a *myo*-inositol transporter in strain RE2. The resulting strain RE2A^{iol} was engineered into an L-lysine producer by introduction of a plasmid carrying the desensitized *lysC*, followed by examination for culture conditions with *myo*-inositol supplementation. We found that as a higher concentration of *myo*-inositol was added to the seed culture, the following fermentation period became shorter while maintaining a high level of L-lysine production. This finally reached a fermentation period comparable to that of the control GapA strain, and yielded a 1.5-fold higher production rate compared with strain RE2. The transcript level of *gapA*, as well as the GapA activity, in the early growth phase increased in proportion to the *myo*-inositol concentration and then fell to low levels in the subsequent growth phase, indicating that improved growth was a result of increased GapA activity, especially in the early growth phase. Moreover, blockade of the pentose phosphate pathway through a defect in glucose 6-phosphate dehydrogenase did not significantly affect L-lysine production in the engineered GapN strains, while a drastic decrease in L-lysine production was observed for the control GapA strain. Determination of the intracellular NADPH/NADP$^+$ ratios revealed that the ratios in the engineered strains were significantly higher than the ratio of the control GapA strain irrespective of the pentose phosphate pathway. These results demonstrate that our strain engineering strategy allows efficient L-lysine production independent of the oxidative pentose phosphate pathway.

Keywords: *Corynebacterium glutamicum*; Glyceraldehyde 3-phosphate dehydrogenases; NADPH; Glycolytic pathway; Pentose phosphate pathway; L-Lysine production

1. Introduction

L-Lysine has been manufactured by the fermentation method using mutants of *Corynebacterium glutamicum*; currently, 2,200,000 tons of L-lysine per year is produced almost exclusively by this method (Eggeling and Bott, 2015). The supply of reducing power, NADPH, is a critical factor for efficient L-lysine production, because 1 mol of L-lysine requires 4 mol of NADPH for its biosynthesis from glucose in *C. glutamicum* (Moritz et al., 2002). It has been reported in this organism that NADPH is generated mainly through the oxidative pentose phosphate pathway (PPP) (Marx et al., 1996). Several reports have shown that redirection of carbon from glycolysis toward the PPP leads to a significant improvement in L-lysine production (Becker et al., 2011, 2007, 2005; Marx et al., 2003; Ohnishi et al., 2005). Despite this positive effect, relying on the PPP is disadvantageous in terms of carbon yield, because the pathway inevitably involves the release of 1 mol of carbon dioxide accompanied by the oxidation of 1 mol of hexose (Contador et al., 2009). This drawback suggests a limitation for using the PPP to produce L-lysine.

Progress in genome science has led to an *in silico* construction of an organism's entire metabolic map. Diverse metabolic pathways of approximately 3,500 bacterial species have already been constructed (Kanehisa et al., 2014; at http://www.kegg.jp/kegg-bin/get_htext?htext=br08601_map00010.keg&hier=5). We noticed using the database that some bacterial species natively lack the complete PPP. Our interest was how such bacteria supply NADPH. Regarding this, *Streptococcus mutans*, which lacks the oxidative part of the PPP because of the absence of two NADP-dependent enzymes, glucose 6-phosphate dehydrogenase (G6PDH) and 6-phosphogluconate dehydrogenase, is known to have a nonphosphorylating NADP-dependent glyceraldehyde 3-phosphate dehydrogenase (GapN) as an alternative source of NADPH (Fig. S1; Crow and Wittenberger, 1979). GapN catalyzes the irreversible oxidation of glyceraldehyde 3-phosphate (GAP) to 3-phosphoglycerate. We conceived that construction of the *S. mutans*-type glycolytic pathway in *C. glutamicum* would remove the need for the PPP, leading to more efficient production of L-lysine and

presumably other NADPH-requiring compounds due to the avoidance of carbon loss through the oxidative PPP.

C. glutamicum ATCC 13032 originally has two glyceraldehyde 3-phosphate dehydrogenases, GapA and GapB. GapA, an NAD-dependent enzyme, is responsible for both glycolysis and gluconeogenesis, and GapB, which represents a dual cofactor signature with a preference for NADP and thus has NADPH-generating potency in the glycolytic direction, works only for gluconeogenesis (Ikeda and Nakagawa, 2003; Takeno et al., 2010). Initially, we isolated the mutants that use GapB for glycolysis from the Δ*gapA* strain. However, the resulting isolates showed insufficient growth on glucose at a level that did not allow for efficient L-lysine production. This suggested that there would be difficulties in exploiting the endogenous enzyme for an NADPH-generating glycolytic pathway. Accordingly, we decided to use the heterologous *S. mutans* GapN enzyme to engineer *C. glutamicum* (Fig. 1). For this purpose, we replaced the deleted *gapA* gene of the Δ*gapAB* double-deleted mutant with the intact *gapN* gene from *S. mutans* to generate a *gapN*-expressing strain, strain GPN (Takeno et al., 2010). Unfortunately, the growth of strain GPN on glucose was significantly retarded despite reconstruction of a functional glycolytic pathway. However, a suppressor mutant with an increased ability to utilize sugars was spontaneously isolated from strain GPN. Analysis of the suppressor mutant RE2 showed that no mutation was present in and upstream of the *gapN* gene, and that the NADP-dependent GapN activity level was unchanged from that of its parental strain GPN (Takeno et al., 2010). Moreover, it was concluded that another mutated enzyme(s) that could functionally substitute for the GapN reaction is most unlikely to emerge in strain RE2 because no suppressor mutant was obtained from Δ*gapAB* strain. Thus, the glycolysis in strain RE2 was concluded to be fully dependent on the NADP-dependent GapN. This suppressor mutant was shown to be a more likely potential host for L-lysine production than the wild-type and Δ*gapB* strains. We also ruled out the possibility that increased L-lysine production is a result of the unknown suppressor mutation(s), by demonstrating using strain RE2A that

replacement of the chromosomal *gapN* gene in strain RE2 with the *gapA* gene reduced L-lysine production to the same level as that of the control Δ*gapB* strain (Takeno et al., 2010). In the present study, the suppressor mutation was identified.

Despite the presence of the suppressor mutation, a limitation of strain RE2 for efficient production is its severely retarded growth relative to the wild-type and Δ*gapB* strains. Here, we show a strategy to shorten the fermentation period of strain RE2 while keeping its high-level L-lysine productivity using GapA only in the early growth phase. In addition, the effect of blocking the PPP through a defect in G6PDH on growth and L-lysine productivity was investigated in the engineered strains.

2. Materials and methods

2.1. Bacterial strains, plasmids, and primers

All strains used in this study are derivative mutants of the wild-type *C. glutamicum* strain ATCC 13032. The Δ*gapB*, GPN, and RE2 strains were previously described (Takeno et al., 2010). In brief, each strain was constructed as follows. The Δ*gapB* strain was constructed by an in-frame deletion of the *gapB* gene in wild-type ATCC 13032. Strain GPN was constructed by replacing the deleted *gapA* gene in the Δ*gapAB* double-deleted mutant of wild-type ATCC 13032 with the intact *gapN* gene from *S. mutans*. Strain RE2, a suppressor mutant with an increased ability to utilize sugars, was spontaneously isolated from strain GPN. *E. coli* DH5α was used as a host for DNA manipulation. Plasmid pCAK311 (Takeno et al., 2010), which contains the desensitized *lysC* gene [*lysC* (T311I)], was used to create L-lysine-producing strains. Plasmid pESB30 (Mitsuhashi et al., 2004), which is nonreplicative in *C. glutamicum*, is a vector for gene replacement in *C. glutamicum*. The primer sequences used in this study are presented in Table S1 in the Supplemental material. All primers were designed based on the genomic sequences of *C. glutamicum* (BA000036) and *S. mutans*

(AE014133), which are publicly available at http://www.genome.jp/kegg/genes.html.

2.2. Media and culture conditions

Minimal medium MM (Takeno et al., 2007), complete medium BY (Takeno et al., 2007), and LFG1 medium for L-lysine production (Takeno et al., 2010) were used to cultivate *C. glutamicum* strains. *C. glutamicum* cells that had been cultured for 1 day on a BY plate containing 20 mg/L of kanamycin were inoculated into 30 mL of BY medium containing glucose and/or *myo*-inositol at the indicated concentrations, 1% $CaCO_3$, and 50 mg/L of kanamycin (seed medium) in a 300-mL baffled Erlenmeyer flask, followed by rotary shaking at 200 rpm. After the glucose initially added into the seed medium was consumed, 3 mL of the seed culture was transferred into 30 mL of LFG1 medium containing 5% glucose, 3% $CaCO_3$, and 200 mg/L of kanamycin in a 300-mL baffled Erlenmeyer flask, followed by rotary shaking at 200 rpm. All cultivations were done at 30ºC.

2.3. Determination of the plasmid maintenance rate

At the end of cultivation for L-lysine production, the cells were diluted at appropriate densities in saline and then plated on kanamycin-free BY agar medium, followed by replication of the emerging cells both on the kanamycin-free and on the kanamycin-containing BY plates. The value was calculated as the rate of the number of kanamycin-resistant isolates to the number of isolates on kanamycin-free BY.

2.4. Recombinant DNA techniques

Standard protocols (Sambrook and Russell, 2001) were used for the construction, purification, and analysis of plasmid DNA and for the transformation of *E.*

coli. The extraction of *C. glutamicum* chromosomal DNA and transformation of *C. glutamicum* by electroporation were performed as described previously (Takeno et al., 2007).

2.5. Identification of a mutation in strain RE2

A suppressor mutation in strain RE2 was identified via a comparative genome analysis with its parental strain GPN. Whole genome sequencing of strains RE2 and GPN was performed by TaKaRa Bio Inc. (Shiga, Japan) using an Illumina Genome Analyzer IIx (Illumina, San Diego, CA).

2.6. Strain construction

For replacement of the chromosomal *iolT1* gene (Cgl0181, NCgl0178) with the homologous *gapA* gene (Cgl1588, NCgl1526), plasmid pCPiolT1-gapA was constructed as follows. The upstream and downstream region of the *iolT1* gene open reading frame (ORF) (for convenience, these regions were referred to as fragments A and B, respectively) were amplified by pairs of primers (the pair comprising Cgl0181delFt and Cgl0181upFusR, and Cgl0181delR and Cgl0181downFusF, respectively), with strain RE2 genomic DNA as a template. The *gapA* gene was amplified by PCR using two primers, GapAFusForf and GapAFusRorf, with the wild-type ATCC 13032 genomic DNA. Fragment A, the *gapA* gene, and fragment B were fused stepwise using PCR. The resulting 2.2-kb fragment was digested with BamHI and then ligated to BamHI-digested pESB30 to yield pCPiolT1-gapA. Defined chromosomal replacement of the *iolT1* gene was accomplished via two recombination events with the plasmid, as described previously (Ohnishi et al., 2002). The resulting strain was designated strain RE2A^{iol}.

For the chromosomal deletion of the *zwf* gene (Cgl1576, NCgl1514), plasmid pCΔzwf, which contains the internally deleted *zwf* gene, was constructed as follows.

The 5’ region of the *zwf* gene was amplified using the primers CGLzwfup200F and zwfFusR, with wild-type ATCC 13032 genomic DNA as the template. Similarly, the 3’ region of the gene was amplified using the primers zwfFusF and CGLzwfdown500R. The 5’ and 3’ regions were fused by PCR using the primers CGLzwfup200F and CGLzwfdown500R. The resulting 1.6-kb fragment contained the deleted *zwf* gene, which was shortened by an in-frame deletion from 1,545 to 831 bp, and thus was devoid of the coding region for its active site (PROSITE motif PS00069). The fragment was digested with BglII and then ligated to BamHI-digested pESB30 to yield pCΔzwf. Defined chromosomal deletion of the *zwf* gene was accomplished via two recombination events with the plasmid.

2.7. RNA extraction, cDNA synthesis, and quantitative PCR

Extraction of total RNAs from *C. glutamicum* strains and subsequent purification were performed according to the methods described previously (Hayashi et al., 2002). Synthesis of cDNA was performed with 300 ng of RNA by the methods described by Kind et al. (2011). Quantitative-PCR (qPCR) analysis was performed by the method described by Katayama et al. (2013). The gene expression levels were standardized to the constitutive level of 16S rRNA expression and calculated by the comparative cycle threshold method (Schmittgen and Livak, 2008).

2.8. Preparation of the soluble fraction and enzyme assays

For GapA and GapN assays, cells at the desired growth phase were collected by centrifugation at 10,000*g* for 10 min and washed twice with 50 mM triethanolamine hydrochloride (pH 8.0) containing 1 mM EDTA and 1mM dithiothreitol. The cells were suspended in 4 volumes of the same buffer and sonicated on ice for 10 min using a UD-200 ultrasonic disruptor (Tomy Seiko Co., Ltd., Tokyo, Japan). Cell debris was

removed by centrifugation at 10,000*g* for 10 min, and the supernatant was further ultracentrifuged at 100,000*g* for 90 min using an Optima TL ultracentrifuge (Beckman Coulter, Inc., Fullerton, CA). The resulting supernatant was provided for GapA and GapN assays. Soluble fractions for the G6PDH assay were prepared using the same method as for GapA and GapN assays except for the buffer, which was 100 mM Tris-HCl (pH 7.5) containing 10 mM $MgCl_2$ and 0.75 mM dithiothreitol. All steps were performed at 4ºC unless otherwise stated. GapA and GapN activities were measured according to the methods described by Omumasaba et al. (2004) and by Crow and Wittenberger (1979), respectively. G6PDH activity was measured according to the method described by Becker et al. (2007). All of the enzyme activities were spectrophotometrically measured using an Ultrospec 3000 spectrophotometer (Amersham Pharmacia Biotech, Cambridge, UK). One unit of activity is defined as 1 μmol of NAD(P)H formed per min.

2.9. Determination of NADPH/NADP+ ratio

One volume of culture broth was mixed with two volumes of cold 60% methanol plus 70 mM HEPES for quenching the intracellular metabolism, according to the methods described previously (Yamauchi et al., 2014; Faijes et al., 2007). Cells were then collected by centrifugation and washed twice with saline, followed by removal of suspended $CaCO_3$ by flash centrifugation. Extraction and determination of intracellular NADPH and $NADP^+$ were performed using an EnzyChrom $NADP^+$/NADPH assay kit (BioAssay System, Hayward, CA).

2.10. Analysis

Bacterial growth was monitored by measuring the optical density at 660 nm (OD_{660}) of the culture broth with a Miniphoto 518R spectrophotometer (Taitec, Saitama,

Japan). Glucose concentration was determined using an F kit D-glucose (Roche Diagnostics, Basel, Switzerland). *Myo*-inositol concentration was determined using a *Myo*-inositol assay kit (Megazyme International Ireland, Wicklow, Ireland). L-Lysine titer was determined as L-lysine HCl, according to the method described by Ohnishi et al. (2005). Protein content was determined using a Bio-Rad protein assay kit (Bio-Rad Laboratories).

3. Results

3.1. Identification of the suppressor mutation in strain RE2

Strain RE2 is a spontaneous suppressor mutant isolated from the culture of strain GPN that has the *S. mutans gapN* gene instead of the native *gapA* and *gapB* genes. While strain GPN showed poor growth on MM medium, strain RE2 exhibited improved growth on the medium (Takeno et al., 2010), and thus, this suppressor mutant is considered to have a particular mutation that confers increased ability to grow on sugar. To identify the mutation, we conducted comparative genomic analysis between strain RE2 and its parental strain GPN. The analysis revealed only one specific mutation, a C-to-T exchange at nucleotide position 2086 in the *rho* gene (Cgl1199, NCgl1152) for the transcription termination factor Rho, which led to the replacement of Arg-696 with Cys (designated mutation *rho696*). Introduction of mutation *rho696* into the strain GPN genome resulted in the same growth profile as strain RE2 in both MM medium and fermentation medium LFG1 containing 5% glucose (data not shown). These results revealed that the suppressor mutation in RE2 is *rho696*.

3.2. Evaluation of strain RE2 as a host for L-lysine production

In our previous report, strain RE2 was found to be a more likely potential host

for L-lysine production than the wild-type and Δ*gapB* strains, based on the final L-lysine titer (Takeno et al., 2010). However, its performance should be evaluated also in terms of the L-lysine production rate (productivity) because the economy of the L-lysine fermentation process depends mainly on the fermentation yield and the productivity of the overall process. To examine the fermentation profile in detail, strain RE2 and the control Δ*gapB* strain were engineered to produce L-lysine by introduction of plasmid pCAK311 [*lysC*(T311I)] (Takeno et al., 2010). The resulting plasmid carriers were cultivated in BY medium containing 2% glucose as a seed culture, followed by cultivation in 30 mL of LFG1 medium containing 5% glucose in 300-mL baffled Erlenmeyer flask (Fig. 2). Under these conditions, strain RE2/pCAK311 produced 2.4-fold more L-lysine (64.4 mM, Fig. 2B) than the control Δ*gapB*/pCAK311 strain (27.1 mM, Fig. 2A), reconfirming that strain RE2 is a high-potential host for L-lysine production. However, strain RE2/pCAK311 required almost 40 h to complete fermentation (Fig. 2G), while the control Δ*gapB*/pCAK311 strain took only 24 h (Fig. 2F). Consequently, the L-lysine production rate in strain RE2/pCAK311 (1.61 mM/h) remains 1.4-fold higher than that of the Δ*gapB*/pCAK311 strain (1.13 mM/h), even though there was a 2.4-fold increase in the final L-lysine titer.

3.3. Further engineering of strain RE2 for more efficient L-lysine production

Although strain RE2 is a high-potential host for L-lysine production, its severely retarded growth despite the suppressor mutation needs to be addressed. Because strain RE2 originates from strain GPN, which was constructed so that the enzymatic steps to generate NADH and ATP (by GapA and the following 3-phosphoglycerate kinase) were replaced with one to generate NADPH only (by GapN; Figs. 1 and 3), this engineering favors the generation of reducing power but is theoretically disadvantageous regarding ATP generation (Fig. 1). Our strategy for solving this problem was to use GapA together with GapN in the early growth phase

where more ATP is required for growth, and thereafter shift the combination-type glycolytic pathway to one that depends only on GapN for production in the subsequent growth phase. This process requires a system to: (i) control the *gapA* expression level or GapA activity at the effective level in the early growth phase; and (ii) reduce them to the lowest possible level in the subsequent growth phase. To develop this process, we planned to use the native promoter of the endogenous *iolT1* gene encoding a *myo*-inositol transporter because the promoter is known to be induced by *myo*-inositol even in the presence of glucose (Krings et al., 2006). In addition, since the inducer *myo*-inositol can be co-metabolized with glucose by *C. glutamicum* (Krings et al., 2006), it is also expected that the *gapA* expression level is reduced during fermentation. Thus, a new strain, strain RE2A^{iol}, was constructed by replacing the chromosomal *iolT1* gene of strain RE2 with the endogenous *gapA* gene (Fig. 3). Although strain RE2A^{iol} lacked the *iolT1* gene, the strain could grow on *myo*-inositol due to the existence of additional transporter encoded by *iolT2* (Cgl3058, NCgl2953). We then examined culture conditions to verify the feasibility of the strategy.

After a variety of examinations, we found that the following combination leads to our desired effective L-lysine production: seed culture grown in BY medium added with *myo*-inositol and then transferred into the main LFG1 medium without *myo*-inositol (Fig. 2). When seed culture that was grown on 2% glucose was used as inoculum, strain RE2A^{iol}/pCAK311 produced a comparable level of L-lysine (68.8 mM, Fig. 2C) for a comparable period (40 h, Fig. 2H), compared with strain RE2/pCAK311 that was precultured under the same conditions (Fig. 2B and G). This suggests that glycolysis is still almost entirely dependent on GapN under these conditions. In contrast, when seed culture that was grown on 2% *myo*-inositol was used as inoculum, strain RE2A^{iol}/pCAK311 required only a 24-h fermentation period (Fig. 2J) and still maintained a high level of L-lysine production (57.8 mM, Fig. 2E), which corresponds to a 2.1-fold higher L-lysine titer than that in the Δ*gapB*/pCAK311 (Fig. 2A and F). On the other hand, when seed culture that was grown on 1.5% glucose plus 0.5%

myo-inositol were used as inoculum, strain RE2A^{iol}/pCAK311 required 32 h (Fig. 2I), and produced 2.4-fold more L-lysine (65.3 mM, Fig. 2D) than the Δ*gapB*/pCAK311 strain. The final L-lysine titers by strain RE2A^{iol}/pCAK311 decreased in a stepwise manner in order of increasing *myo*-inositol concentration in the seed medium, whereas its L-lysine production rate increased in the opposite order as follows: 1.72 mM/h for 2% glucose, 2.04 mM/h for 1.5% glucose plus 0.5% *myo*-inositol, and 2.41 mM/h for 2% *myo*-inositol. *Myo*-inositol that was carried over to the main medium at different concentrations slowly decreased from the beginning of the cultivation (Fig. 2I and J). Such a decline in *myo*-inositol starting from the early growth phase was judged to be beneficial to our strategy to reduce the *gapA* expression level in the rest of the growth phase. The plasmid maintenance rate at the end of cultivation was more than 97.0% in all cultures shown in Fig. 2. Next, we verified whether these positive results were derived in accordance with our intention.

3.4. The gapA and gapN transcript levels during L-lysine production

We conducted a time-course analysis of *gapA* and *gapN* transcript levels in strain RE2A^{iol}/pCAK311 during L-lysine production (Fig. 4). The data for *gapA* and *gapN* are presented as relative values to those obtained for the corresponding genes at 8 h in the control strains Δ*gapB*/pCAK311 (for *gapA*) and RE2/pCAK311 (for *gapN*), respectively, both of which were obtained using seed culture on glucose. The *gapA* transcript levels in the control strain Δ*gapB*/pCAK311 (Fig. 4A) and the *gapN* transcript levels in the other control strain RE2/pCAK311 (Fig. 4B) were generally higher in the early growth phase than in the following growth phase and then decreased gradually as the growth proceeded. A similar pattern was also observed for *gapN* in the newly engineered strain RE2A^{iol}/pCAK311, regardless of the seed culture conditions (Fig. 4C-E). These data indicate that our selected conditions do not substantially influence *gapN* expression in itself. However, the *gapA* transcript level in strain

RE2A^{iol}/pCAK311 differed depending on the seed culture conditions with different composition of glucose and *myo*-inositol. For glucose only (2%), the *gapA* transcript level was at the basal level throughout the cultivation (Fig. 4C). However, for *myo*-inositol only (2%), the *gapA* transcript level was maximal in the early exponential phase (at 8 h), which corresponds to approximately 60% of the control value, and thereafter fell to remarkably low levels in the mid-exponential phase (at 16 h; Fig. 4E). On the other hand, for glucose (1.5%) plus *myo*-inositol (0.5%), the *gapA* transcript level was similarly maximal in the early exponential phase (at 8 h), which is approximately 27% of the control value, and it then fell to the same basal level as observed for glucose in the mid-exponential phase (at 16 h; Fig. 4D). These data indicate that the *gapA* expression level in the early exponential phase is controlled by *myo*-inositol in a dose-dependent manner under the coexistence of glucose, and it is reduced to low levels in the mid-exponential phase as *myo*-inositol decreases.

3.5. The GapA and GapN enzymatic activities during L-lysine production

Besides the transcript levels, GapA and GapN activities during L-lysine production were determined (Table 1). Whereas NADP-dependent GapN activities in strain RE2A^{iol}/pCAK311 and in strain RE2/pCAK311 were not substantially different in each corresponding growth phase regardless of the seed culture conditions, NAD-dependent GapA activities in strain RE2A^{iol}/pCAK311 were clearly different among the seed culture conditions. For glucose only, GapA activity was not detected in strain RE2A^{iol}/pCAK311. However, for glucose plus *myo*-inositol, GapA activity was detected at a relatively moderate level in the early exponential phase (181.8 mU/mg at 8 h) but it was absent in the mid-exponential phase (at 16 h). On the other hand, for *myo*-inositol only, GapA activity was remarkably high in the early exponential phase (571.9 mU/mg at 8 h) and declined to low levels in the mid-exponential phase (58.2 mU/mg at 16 h). These data, together with the gene expression data (Fig. 4), show that

the *gapA* transcript level was positively correlated with GapA activity and that the elevated growth rate of strain RE2A^{iol}/pCAK311 by *myo*-inositol supplementation was accompanied by increasing GapA activity, especially in the early exponential phase.

3.6. Effect of zwf disruption on L-lysine production

As described in the introduction, contribution of the PPP to L-lysine production was thought to be insignificant in strain RE2, and also presumably in strain RE2A^{iol}. Even though carbon flux analysis was one of the methods of verifying the hypothesis, we selected a more direct method, by which effect of blocking the oxidative PPP on L-lysine production was investigated. If the hypothesis is true, the PPP blockade has no impact on or hardly affects L-lysine production by strain RE2/pCAK311 and RE2A^{iol}/pCAK311. Thus, PPP mutants, strains RE2Δ*zwf* and RE2A^{iol}Δ*zwf*, together with the Δ*gapB*Δ*zwf* strain as a control, were constructed by in-frame deletion of the chromosomal *zwf* gene encoding G6PDH. The soluble fractions from the *zwf*-disrupted strains Δ*gapB*Δ*zwf*/pCAK311, RE2Δ*zwf*/pCAK311, and RE2A^{iol}Δ*zwf*/pCAK311 exhibited no G6PDH activity, whereas those from strains Δ*gapB*/pCAK311, RE2/pCAK311, and RE2A^{iol}/pCAK311 showed G6PDH activities of 94.4 mU/mg, 84.5 mU/mg, and 123.5 mU/mg, respectively.

The resulting strains were examined for their growth properties and L-lysine production (Fig. 2). Deletion of the *zwf* gene in the Δ*gapB*/pCAK311 strain reduced its L-lysine level by approximately 60% (Fig. 2A), and caused a lower growth level and prolongation of the cultivation period to 32 h (Fig. 2F). However, the gene deletion in strain RE2 hardly affected both L-lysine production and growth (Fig. 2B and G). The same results were obtained in strain RE2A^{iol}/pCAK311 for the seed culture conditions with glucose only (Fig. 2C and H) and with glucose plus *myo*-inositol (Fig. 2D and I). These data demonstrate that the oxidative PPP is, as expected, unnecessary for L-lysine production by these strains. Meanwhile, somewhat obvious decrease in the final

L-lysine titer by deletion of the *zwf* gene was observed for the seed culture conditions with *myo*-inositol only (Fig. 2E). Considering the slower production rate of L-lysine in the early exponential phase compared with that in the subsequent growth phase, it is likely that the induced GapA activity in the early exponential phase raised the need for NADPH through the PPP, especially in the early exponential phase.

3.7. Intracellular NADPH/NADP$^+$ ratio during L-lysine production

Although L-lysine production by strains RE2/pCAK311 and RE2A^{iol}/pCAK311 were well over 2.0-fold higher than that by the control Δ*gapB*/pCAK311 strain, avoidance of carbon loss resulting from bypassing the PPP alone never explains the marked increase beyond 1.2-fold as a theoretical maximum. Thus, we hypothesized that the NADPH-generating glycolytic pathway using GapN would give rise to elevated NADPH levels, which resulted in acceleration of L-lysine biosynthesis. To verify this hypothesis, the intracellular NADPH/NADP$^+$ ratio was determined using cells grown to the mid-exponential phase. Culture conditions for each strain were identical to those performed in Fig. 2. The ratio was 0.329±0.01 for the Δ*gapB*/pCAK311 strain (at 16 h). On the other hand, the ratio in either strain RE2/pCAK311 or strain RE2A^{iol}/pCAK311 irrespective of seed culture conditions was significantly higher than that obtained by the Δ*gapB*/pCAK311 strain. It was 0.533±0.08 in strain RE2/pCAK311 (at 24 h), 0.570±0.03 in strain RE2A^{iol}/pCAK311 for glucose (at 32 h), 0.526±0.08 in strain RE2A^{iol}/pCAK311 for glucose plus *myo*-inositol (at 16 h), and 0.445±0.01 in strain RE2A^{iol}/pCAK311 for *myo*-inositol only (at 16 h). These values are correlated with L-lysine production shown in Fig. 2, which almost has a quantitative relationship.

Deletion of *zwf* has little to no influence on L-lysine production by strains RE2/pCAK311 and RE2A^{iol}/pCAK311 (Fig. 2). Based on the above hypothesis, these results should accompany the same degree of the higher NADPH/NADP$^+$ ratio as those obtained for their parental *zwf*-positive strains. To further verify the hypothesis, the

NADPH/$NADP^+$ ratio was determined for strains RE2Δ*zwf*/pCAK311 and $RE2A^{iol}$Δ*zwf*/pCAK311. The ratios were, as expected, comparable to those obtained for their corresponding parental strains: 0.645±0.06 for strain RE2Δ*zwf*/pCAK311 (at 24 h), 0.603±0.00 in strain $RE2A^{iol}$Δ*zwf*/pCAK311 for glucose (at 24 h), 0.571±0.02 in strain $RE2A^{iol}$Δ*zwf*/pCAK311 for glucose plus *myo*-inositol (at 16 h), and 0.468±0.01 in strain $RE2A^{iol}$/pCAK311 for *myo*-inositol only (at 16 h). These results not only confirm that the PPP is insignificant for NADPH regeneration in these strains but also support our hypothesis that the NADPH-generating glycolytic pathway would direct cells to a highly reduced state, which allows the cells to overproduce L-lysine.

4. Discussion

We showed that the suppressor mutant RE2, which mainly generates NADPH through the glycolytic pathway, is a high-potential host for L-lysine production. The suppressor mutation was elucidated to be a point mutation in the *rho* gene (*rho696*). However, despite the presence of the mutation, strain RE2 still showed a lower growth rate on glucose than the wild-type and Δ*gapB* strains. This drawback was overcome by taking advantage of GapA using the *myo*-inositol-inducible expression system in combination with simple seed culture conditions. This engineering led to improved growth while maintaining higher L-lysine productivity: strain $RE2A^{iol}$/pCAK311 showed an approximately 1.3- to 1.5-fold higher production rate than did strain RE2/pCAK311 (Fig. 2B, D and E), which was approximately 1.8- to 2.1-fold higher than the Δ*gapB*/pCAK311 strain (Fig. 2A, D and E). The elevated growth rate was shown to be accompanied by increasing GapA activity, especially in the early exponential phase (Table 1). The most noteworthy achievement in the present study was that, unlike in the control Δ*gapB*/pCAK311 strain, the oxidative PPP blockade by the *zwf* gene deletion had little to no effect on both L-lysine production and the fermentation period in strains RE2/pCAK311 and $RE2A^{iol}$/pCAK311 (Fig. 2), demonstrating that the

oxidative PPP is not significant in these strains. Therefore, we conclude that the NADPH-generating glycolytic pathway using GapN eliminates the need for the oxidative PPP in the efficient production of L-lysine by *C. glutamicum*. Considering that 4 mol of NADPH is required for 1 mol of L-lysine production, and also that 2 mol of NADPH is inevitably generated from 1 mol of glucose at the GapN step, the engineered GapN strains can theoretically supply the NADPH required for L-lysine biosynthesis up to a yield of 0.5 mol L-lysine/mol of sugar, regardless of the flux distribution between glycolysis and the PPP. Because the L-lysine yields by the GapN strains are still below the theoretical upper limit, the GapN strains are thought to supply a sufficient amount of NADPH to its L-lysine biosynthesis through the reconstructed glycolytic pathway without depending on the PPP. This study is the first to demonstrate efficient L-lysine production independent of the oxidative PPP. The results of the present study are summarized in Fig. 5.

The suppressor mutation *rho696*, which led to the replacement of Arg-696 with Cys in the transcription termination factor Rho protein, improved the growth of strain GPN on glucose. This was confirmed not only by the whole genomic analysis of the suppressor mutant RE2 but also introduction of the mutation into the parental strain GPN. However, causal effects of *rho696* on the growth improvement remain to be elucidated. Homology analysis provided the following information: i) Arg-696 is located in the C-terminal region of *C. glutamicum* Rho where there is a highly conserved region among a wide variety of bacterial Rho proteins, including those of *E. coli* and *Bacillus subtilis*; and ii) the Arg-696 residue is strictly conserved among bacterial Rho and also corresponds to an Arg residue at amino acid position 366 in *E. coli* Rho. It has been reported in *E. coli* Rho that replacement of the Arg-366 with His causes a complete defect in transcription termination *in vivo* because of a severe decrease in its RNA-dependent ATPase activity (Miwa et al., 1995). Therefore, the *rho696* mutation is likely to damage Rho transcription termination activity. Moreover, it has been reported in *E. coli* Rho that defects in termination cause a 10- to 20-fold

increase in read-through efficiency (Chalissery et al., 2007). Therefore, increased expression of a certain gene(s) is possibly caused by read-through transcription over the Rho-dependent transcription termination site because of *rho*696, and among such gene(s), there seems to be a candidate(s) to make the GapN-dependent glycolytic pathway work more efficiently. Recently, it has been reported that the severe growth defect of the high NADPH-generating *C. glutamicum* strain, where the *pgi* gene encoding the phosphoglucose isomerase was deleted, is not caused by increased intracellular NADPH concentrations, as previously predicted, but by the negative effect on glucose uptake, which is caused by a strongly reduced level of PtsG component in phosphotransferase system (PTS) by a still-unknown mechanism (Lindner et al., 2013). It is not unreasonable for these findings to be applied to our high NADPH-generating strain. Thus, *rho696* might cause increased levels of PtsG and/or balance the intracellular amount of phosphoenolpyruvate and pyruvate, which are the substrate and product for PTS, respectively, to support the PTS-dependent glucose uptake.

Very recently, it was reported that *Clostridium acetobutylicum gapN* expression does not allow the *C. glutamicum* ATCC 13032 Δ*gapAB* strain to grow in glucose minimal medium (Komati Reddy et al., 2015). All four suppressor mutants obtained by these researchers shared only one specific mutation: a single point mutation in the *ndh* gene encoding non-proton-pumping NADH:ubiquinone oxidoreductase (NDH-II), which leads to the amino acid change D213G. The mutated NDH-II was shown *in vitro* to oxidize NADH and also NADPH. They reasonably concluded that the growth inhibition in their *gapN*-expressing strain was a result of excess NADPH and that the mutation is responsible for oxidation of NADPH to $NADP^+$ coupled with electron transport phosphorylation, resulting in ATP generation. Taking their results into consideration, mutation *rho696* should likely be dealt with from NADPH reoxidation and/or ATP generation. However, in our case, it is difficult to suppose that mutation *rho696* causes NADPH reoxidation to $NADP^+$, because no growth improvement in strain GPN was observed by engineering for L-lysine overproduction, i.e., by

construction of the pathway that consumes a large amount of NADPH (Takeno et al., 2010). Thus, we suggest that mutation *rho696* leads to improved ATP generation rather than to NADPH reoxidation. It should be noted that, besides bypassing ATP generation in the glycolysis, metabolic engineering using GapN is likely to reduce carbon flux through the TCA cycle and thereby to decrease NADH supply for ATP generation by oxidative phosphorylation. This point is discussed later, again.

The growth of strain RE2A^{iol}/pCAK311 was gradually improved as GapA activity was increased, especially in the early exponential phase (Fig. 2H-J and Table 1). Although improved growth still maintains the high L-lysine productivity, the GapA activity was somewhat negatively correlated with final L-lysine production (Fig. 2C-E), suggesting that use of GapA causes the decrease in NADPH supply. Actually, the NADPH/NADP$^+$ ratio in strain RE2A^{iol}/pCAK311 was relatively lower under conditions where the GapA activity was present (the ratio of 0.445±0.01) compared with when no GapA activity was observed (the ratio of 0.526±0.08 to 0.570±0.03). The reasonable explanation is that the increased involvement of GapA in glycolysis leads to growth improvement, presumably because of ATP generation, but concomitantly reduces GAP availability for GapN, resulting in a decrease in the NADPH supply. Considering that excessive dependency on GapA negatively affects L-lysine production in the engineered GapN strains, the advantage of the system developed in the present study is to allow cells to reconcile growth with lysine production in a well-balanced state.

It is also worth noting that the glycolytic pathway using GapN leads to efficient L-lysine production independent of the oxidative PPP, which was verified by confirming that blocking the oxidative PPP by deleting the *zwf* gene has little effect both on L-lysine production and on the high NADPH/NADP$^+$ ratio in either strains RE2/pCAK311 or RE2A^{iol}/pCAK311 (Fig. 2B-E). Recently, it has been reported that the engineering of the *C. glutamicum* glycolytic pathway using a modified GapA variant that showed a preference toward both NAD$^+$ and NADP$^+$ resulted in increased L-lysine

production (1.25- to 1.65-fold higher production). However, this barely changed carbon fluxes through the PPP (Bommareddy et al., 2014), suggesting that remnant of NAD-reactive properties of GapA inevitably draws the necessity of the PPP. Similar results might be seen for strain RE2A^{iol}/pCAK311 in the early exponential phase where considerable GapA activity coexisted with GapN (Fig. 2E). Under these conditions, the PPP blockade has a somewhat distinguishable impact on L-lysine production. Besides engineering for redirection of carbon toward the PPP, the heterologous expression of *pntAB* genes, which encode a membrane-bound transhydrogenase catalyzing the interconversion of NADH and NADPH, increases L-lysine production on glucose; however, the PPP has been suggested to still contribute to the sufficient NADPH supply (Kabus et al., 2007).

In this study, construction of *S. mutans*-type glycolytic pathway in *C. glutamicum* has led to an impressive result in L-lysine production. The better-than-expected result seems to be partly due to the avoidance of carbon loss through the oxidative PPP, but rather due to the increased intracellular NADPH/NADP$^+$ ratio. It has been reported that, on fructose compared with on glucose, carbon flux through the PPP is significantly decreased (62.0% to 14.4%), and that through the TCA cycle is increased (52.9% to 83.3%) for a partial compensation of the anabolic NADPH requirement (Kiefer et al., 2004). Considering conversely, carbon flux through the TCA cycle is likely reduced in our high NADPH-generating strain. In fact, deletion of phosphoglucose isomerase, which is the radical strategy for NADPH supply by which almost all glucose fluxes through the PPP, decreased the flux through the TCA cycle during L-lysine production (Marx et al., 2003). Therefore, it seems reasonable to consider that the high NADPH/NADP$^+$ ratio obtained in the present study not only allows cells to bypass the PPP but also causes a decreased flux through the TCA cycle. This would cause increased availability of oxaloacetate supplied through anaplerotic pathways and result in augmented L-lysine biosynthesis.

As shown here for L-lysine, the strain engineered to generate NADPH through

glycolysis is likely to be an effective host for other NADPH-requiring compounds, such as other amino acids (Ikeda and Takeno, 2013), commodity chemicals (Kind et al., 2011; Song et al., 2013), vitamins (Hüser et al., 2005; Ikeda et al., 2013), fatty acids (Takeno et al., 2013), and carotenoids (Heider et al., 2012). The results of the present study will pave the way for efficient production of these compounds.

Acknowledgements

We thank Yasuo Ueda and Shin-ichi Hashimoto for their encouraging support of our research.

References

Becker, J., Klopprogge, C., Herold, A., Zelder, O., Bolten, C.J., Wittmann, C., 2007. Metabolic flux engineering of L-lysine production in *Corynebacterium glutamicum*—over expression and modification of G6P dehydrogenase. J. Biotechnol. 132, 99-109.

Becker, J., Klopprogge, C., Zelder, O., Heinzle, E., Wittmann, C., 2005. Amplified expression of fructose 1,6-bisphosphatase in *Corynebacterium glutamicum* increase *in vivo* flux through the pentose phosphate pathway and lysine production on different carbon sources. Appl. Environ. Microbiol. 71, 8587-8596.

Becker, J., Zelder, O., Häfner, S., Schröder, H., Wittmann, C., 2011. From zero to hero—Design-based systems metabolic engineering of *Corynebacterium glutamicum* for L-lysine production. Metab. Eng. 13, 159-168.

Bommareddy, R.R., Chen, Z., Rappert, S., Zeng, A.P., 2014. A *de novo* NADPH generation pathway for improving lysine production of *Corynebacterium glutamicum* by rational design of the coenzyme specificity of glyceraldehyde 3-phosphate dehydrogenase. Metab. Eng. 25, 30-37.

Chalissery, J., Banerjee, S., Bandey, I., Sen, R., 2007. Transcription termination

defective mutants of Rho: role of different functions of Rho in releasing RNA from the elongation complex. J. Mol. Biol. 371, 855-872.

Contador, C.A., Rizk, M.L., Asenjo, J.A., Liao, J.C., 2009. Ensemble modeling for strain development of L-lysine-producing *Escherichia coli*. Metab. Eng. 11, 221-233.

Crow, V.L., Wittenberger, C.L., 1979. Separation and properties of NAD^+- and $NADP^+$-dependent glyceraldehyde-3-phosphate dehydrogenases from *Streptococcus mutans*. J. Biol. Chem. 254, 1134-1142.

Eggeling, L., Bott, M., 2015. A giant market and a powerful metabolism: L-lysine provided by *Corynebacterium glutamicum*. Appl. Microbiol. Biotechnol. 99, 3387-3394.

Faijes, M., Mars, A.E., Smid, E.J., 2007. Comparison of quenching and extraction methodologies for metabolome analysis of *Lactobacillus plantarum*. Microb. Cell Fact. 6, 27.

Hayashi, M., Mizoguchi, H., Shiraishi, N., Obayashi, M., Nakagawa, S., Imai, J., Watanabe, S., Ota, T., Ikeda, M., 2002. Transcriptome analysis of acetate metabolism in *Corynebacterium glutamicum* using a newly developed metabolic array. Biosci. Biotechnol. Biochem. 66, 1337-1344.

Heider, S.A.E., Peters-Wendisch, P., Wendisch, V.F., 2012. Carotenoid biosynthesis and overproduction in *Corynebacterium glutamicum*. BMC Microbiol. 12, 198

Hüser, A.T., Chassagnole, C., Lindley, N.D., Merkamm, M., Guyonvarch, A., Elišáková, V., Pátek, M., Kalinowski, J., Brune, I., Pühler, A., Tauch, A., 2005. Rational design of a *Corynebacterium glutamicum* pantothenate production strain and its characterization by metabolic flux analysis and genome-wide transcriptional profiling. Appl. Environ, Microbiol. 71, 3255-3268.

Ikeda, M., Miyamoto, A., Mutoh, S., Kitano, Y., Tajima, M., Shirakura, D., Takasaki, M., Mitsuhashi, S., Takeno, S., 2013. Development of biotin-prototrophic and -hyperauxotrophic *Corynebacterium glutamicum*. Appl. Environ. Microbiol. 79,

4586-4594.

Ikeda, M., Nakagawa, S., 2003. The *Corynebacterium glutamicum* genome: features and impacts on biotechnological processes. Appl. Microbiol. Biotechnol. 62, 99-109.

Ikeda, M., Takeno, S., 2013. Amino acid production by *Corynebacterium glutamicum*. In: Yukawa, H., Inui, M. (Eds.), *Corynebacterium glutamicum*. Microbiology monographs, vol. 23. Springer, Berlin, Germany, pp. 107-147.

Kabus, A., Georgi, T., Wendisch V.F., Bott, M., 2007. Expression of the *Escherichia coli pntAB* genes encoding a membrane-bound transhydrogenase in *Corynebacterium glutamicum* improves L-lysine formation. Appl. Microbiol. Biotechnol. 75, 47-53.

Kanehisa, M., Goto, S., Sato, Y., Kawashima, M., Furumichi, M., Tanabe, M., 2014. Data, information, knowledge and principle: back to metabolism in KEGG. Nucleic Acids Res. 42, D199-D205.

Katayama, S., Kukita, T., Ishikawa, E., Nakashima, S., Masuda, S., Kanda, T., Akiyama, H., Teshima, R., Nakamura, S., 2013. Apple polyphenols suppress antigen presentation of ovalbumin by THP-1-derived dendritic cells. Food Chem. 138, 757-761.

Kiefer, P., Heinzle, E., Zelder, O., Wittmann, C., 2004. Comparative metabolic flux analysis of lysine-producing *Corynebacterium glutamicum* cultured on glucose or fructose. Appl. Environ. Microbiol. 70, 229-239.

Kind, S., Kreye, S., Wittmann, C., 2011. Metabolic engineering of cellular transport for overproduction of the platform chemical 1,5-diaminopentane in *Corynebacterium glutamicum*. Metab. Eng. 13, 617-627.

Komati Reddy, G., Lindner, S.N., Wendisch, V.F., 2015. Metabolic engineering of an ATP-neutral Embden-Meyerhof-Parnas pathway in *Corynebacterium glutamicum*: growth restoration by an adaptive point mutation in NADH dehydrogenase. Appl. Environ. Microbiol. 81, 1996-2005.

Krings, E., Krumbach, K., Bathe, B., Kelle, R., Wendisch, V.F., Sahm, H., Eggeling, L.,

2006. Characterization of *myo*-inositol utilization by *Corynebacterium glutamicum*: the stimulon, identification of transporters, and influence on L-lysine formation. J. Bacteriol. 188, 8054-8061.

Lindner, S.N., Petrov, D.P., Hagmann, C.T., Henrich, A., Krämer, R., Eikmanns, B.J., Wendisch, V.F., Seibold, G.M., 2013. Phosphotransferase system-mediated glucose uptake is repressed in phosphoglucoisomerase-deficient *Corynebacterium glutamicum* strains. Appl. Environ. Microbiol. 79, 2588-2595.

Marx, A., Hans, S., Möckel, B., Bathe, B., de Graaf, A.A., 2003. Metabolic phenotype of phosphoglucose isomerase mutants of *Corynebacterium glutamicum*. J. Biotechnol. 104, 185-197.

Marx, A., de Graaf, A.A., Wiechert, W., Eggeling, L., Sahm, H., 1996. Determination of the fluxes in the central metabolism of *Corynebacterium glutamicum* by nuclear magnetic resonance spectroscopy combined with metabolite balancing. Biotechnol. Bioeng. 49, 111-129.

Mitsuhashi, S., Ohnishi, J., Hayashi, M., Ikeda, M., 2004. A gene homologous to β-type carbonic anhydrase is essential for the growth of *Corynebacterium glutamicum* under atmospheric conditions. Appl. Microbiol. Biotechnol. 63, 592-601.

Miwa, Y., Horiguchi, T., Shigesada, K., 1995. Structural and functional dissections of transcription termination factor Rho by random mutagenesis. J. Mol. Biol. 254, 815-837.

Moritz, B., Striegel, K., de Graaf, A.A., Sahm, H., 2002. Changes of pentose phosphate pathway flux *in vivo* in *Corynebacterium glutamicum* during leucine-limited batch cultivation as determined from intracellular metabolite concentration measurements. Metab. Eng. 4, 295-305.

Ohnishi, J., Katahira, R., Mitsuhashi, S., Kakita, S., Ikeda, M., 2005. A novel *gnd* mutation leading to increased L-lysine production in *Corynebacterium glutamicum*. FEMS Microbiol. Lett. 242, 265-274.

Ohnishi, J., Mitsuhashi, S., Hayashi, M., Ando, S., Yokoi, H., Ochiai, K., Ikeda, M.,

2002. A novel methodology employing *Corynebacterium glutamicum* genome information to generate a new L-lysine-producing mutant. Appl. Microbiol. Biotechnol. 58, 217-223.

Omumasaba, C.A., Okai, N., Inui, M., Yukawa, H., 2004. *Corynebacterium glutamicum* glyceraldehyde-3-phosphate dehydrogenase isoforms with opposite, ATP-dependent regulation. J. Mol. Microbiol. Biotechnol. 8, 91-103.

Sambrook, J., Russell, D.W., 2001. Molecular cloning: a laboratory manual, third ed. Cold Spring Harbor Laboratory Press, Cold Spring Harbor, New York

Schmittgen, T.D., Livak, K.J., 2008. Analyzing real-time PCR data by the comparative C_T method. Nat. Protoc. 3, 1101-1108.

Song, Y., Matsumoto, K., Tanaka, T., Kondo, A., Taguchi, S., 2013. Single-step production of polyhydroxybutyrate from starch by using α-amylase cell-surface displaying system of *Corynebacterium glutamicum*. J. Biosci. Bioeng. 115, 12-14.

Takeno, S., Murata, R., Kobayashi, R., Mitsuhashi, S., Ikeda, M., 2010. Engineering of *Corynebacterium glutamicum* with an NADPH-generating glycolytic pathway for L-lysine production. Appl. Environ. Microbiol. 76, 7154-7160.

Takeno, S., Ohnishi, J., Komatsu, T., Masaki, T., Sen, K., Ikeda, M., 2007. Anaerobic growth and potential for amino acid production by nitrate respiration in *Corynebacterium glutamicum*. Appl. Microbiol. Biotechnol. 75, 1173-1182.

Takeno, S., Takasaki, M., Urabayashi, A., Mimura, A., Muramatsu, T., Mitsuhashi, S., Ikeda, M., 2013. Development of fatty acid-producing *Corynebacterium glutamicum* strains. Appl. Environ. Microbiol. 79, 6776-6783.

Yamauchi, Y., Hirasawa, T., Nishii, M., Furusawa, C., Shimizu, H., 2014. Enhanced acetic acid and succinic acid production under microaerobic conditions by *Corynebacterium glutamicum* harboring *Escherichia coli* transhydrogenase gene *pntAB*. J. Gen. Appl. Microbiol. 60, 112-118.

Figure Legends

Fig. 1. Glycolytic pathways and the pentose phosphate pathways in strain RE2 (right) and its parental Δ*gapB* strain (left). Strain RE2, a suppressor mutant from strain GPN, has a glycolytic pathway that was constructed by replacing its intrinsic NAD-dependent glyceraldehyde 3-phosphate dehydrogenase (GapA) with a non-phosphorylating NADP-dependent glyceraldehyde 3-phosphate dehydrogenase (GapN) from *S. mutans*. The engineering leads to NADPH generation via the glycolytic process but instead bypassing ATP generation. Arrows with solid and dotted lines represent single and multiple enzymatic processes, respectively. Abbreviations are as described in the legend to Fig. S1.

Fig. 2. L-lysine production and growth in strains RE2/pCAK311 and RE2Δ*zwf*/pCAK311 (B and G), strains RE2A^{iol}/pCAK311 and RE2A^{iol}Δ*zwf*/pCAK311 (C-E and H-J), and the control Δ*gapB*/pCAK311 and Δ*gapB*Δ*zwf*/pCAK311 strains (A and F). All strains were cultivated in 30 mL of LFG1 medium containing 5% glucose in a 300-mL baffled Erlenmeyer flask at 30ºC with rotary shaking at 200 rpm. The preceding seed culture conditions for each strain were as follows: BY medium containing 2% glucose (A-C and F-H), BY medium containing 1.5% glucose plus 0.5% *myo*-inositol (D and I), and BY medium containing 2% *myo*-inositol (E and J). White and black symbols represent data for strains with the intact *zwf* gene and the deletants of *zwf*, respectively. *Myo*-inositol presented in (I) and (J) was the carry-over from the seed culture. Values are means of replicated cultures, which showed <5% difference from each other.

Fig. 3. Construction of strain RE2A^{iol}. Strain RE2A^{iol} was constructed from strain RE2 by replacing the genomic *iolT1* open reading frame (ORF) with the endogenous *gapA* ORF. All strains used in this study are also presented.

Fig. 4. Relative transcript levels of *gapA* and *gapN* during L-lysine production. Total RNAs were prepared from cells of the indicated times of L-lysine production shown in Fig. 2. Aliquots of RNAs were reverse transcribed and subjected to qPCR. The transcript levels of *gapN* (black bars) and *gapA* (white bars) were standardized to the constitutive expression level of 16S rRNA, and are presented as relative values to those obtained for the corresponding genes at 8 h in the Δ*gapB*/pCAK311 strain (for *gapA*) (A) and strain RE2/pCAK311 (for *gapN*) (B), respectively. The data for the Δ*gapB*/pCAK311 strain that was precultured on 2% glucose is presented in (A), for strain RE2/pCAK311 that was precultured on 2% glucose is presented in (B), for strain RE2A^{iol}/pCAK311 that was precultured on 2% glucose is presented in (C), for strain RE2A^{iol}/pCAK311 that was precultured on 1.5% glucose plus 0.5% *myo*-inositol is presented in (D), and for strain RE2A^{iol}/pCAK311 that was precultured on 2% *myo*-inositol is presented in (E). Data represent mean value from three independent cultures, and the standard deviation from the mean is indicated as error bars.

Fig. 5. Summary of this work. Growth retardation of strain RE2 was overcome while maintaining its high ability to produce L-lysine using GapA at an effective level in the early exponential phase. Decline in GapA activity from the early to mid-exponential phase is represented with a gradational arrow in strain RE2A^{iol} (rightmost). The best result of strain RE2A^{iol} in terms of production rate was obtained using seed culture on 2% *myo*-inositol. In this condition, the newly engineered strain gave 2.1-fold higher L-lysine titer than the control Δ*gapB*/pCAK311 strain for a comparable period, and yielded a production rate of 2.41 mM/h. In conclusion, well-balanced use of GapA and GapN in strain RE2A^{iol} led to both improved growth and high-level L-lysine production that is independent of the PPP. Abbreviations are as described in the legend to Fig. S1.

Table 1 Specific activities of GapA and GapN in the engineered *C. glutamicum* strains.

Strain	Carbon source in seed culture	Enzyme activity (mU/mg)							
		Early exponential phase				Mid-exponential phase			
		GapA		GapN		GapA		GapN	
		NAD^+	$NADP^+$	NAD^+	$NADP^+$	NAD^+	$NADP^+$	NAD^+	$NADP^+$
Δ*gapB*/pCAK311	Glucose	1645.1 ± 64.6	–	ND	ND	1224.6 ± 79.7	–	ND	ND
RE2/pCAK311	Glucose	ND	ND	18.7 ± 6.3	845.7 ± 6.9	ND	ND	11.1 ± 3.8	310.5 ± 57.0
$RE2A^{iol}$/pCAK311	Glucose	–	ND	32.7 ± 19.6	724.8 ± 66.5	–	ND	6.7 ± 2.3	344.1 ± 45.1
	Glucose + *Myo*-inositol	181.8 ± 12.9	ND	ND	462.3 ± 38.2	–	ND	ND	317.5 ± 32.8
	Myo-inositol	571.9 ± 21.1	ND	ND	460.8 ± 19.8	58.2 ± 7.4	ND	ND	331.2 ± 112.1

Data represent mean values and standard deviations of three independent cultures. –, not detected; ND, not determined.

Highlights

- Growth of the *C. glutamicum* strain with *S. mutans gapN* was improved by growth phase-specific induction of endogenous *gapA*.
- The engineered GapN strain achieved a 1.8- to 2.1-fold higher L-lysine production rate than the control GapA strain.

- The efficient production was demonstrated to be independent of the oxidative pentose phosphate pathway.
- Intracellular NADPH/$NADP^+$ ratio of the GapN strain during L-lysine production was significantly higher than that of the GapA strain.

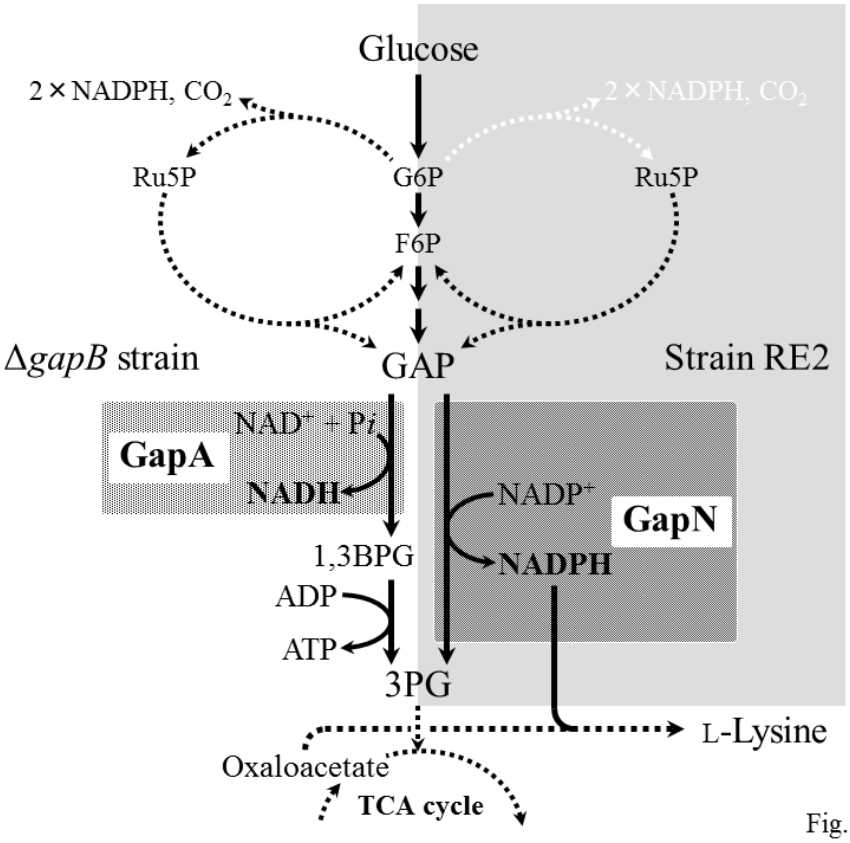

Fig. 1. Takeno

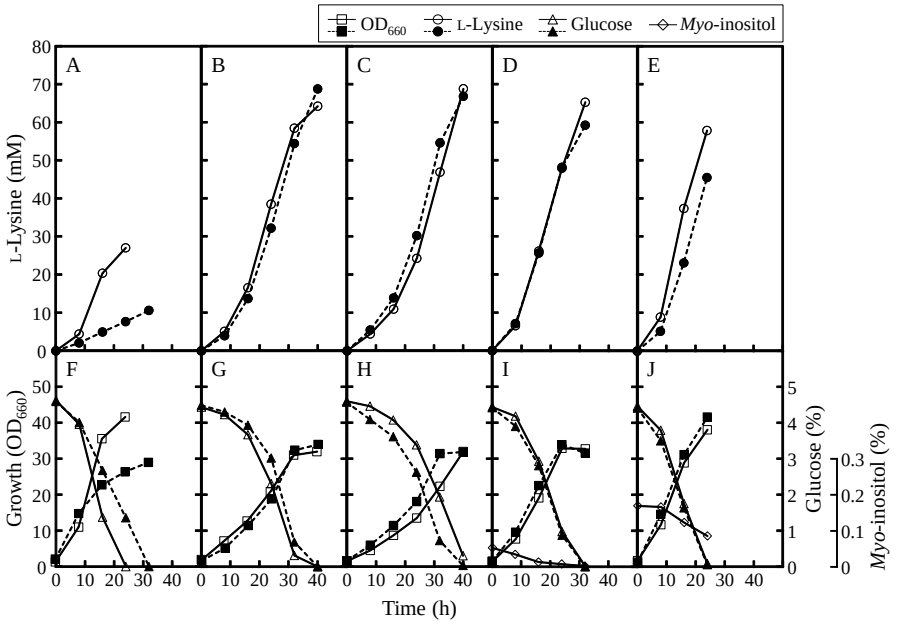

Fig. 2. Takeno

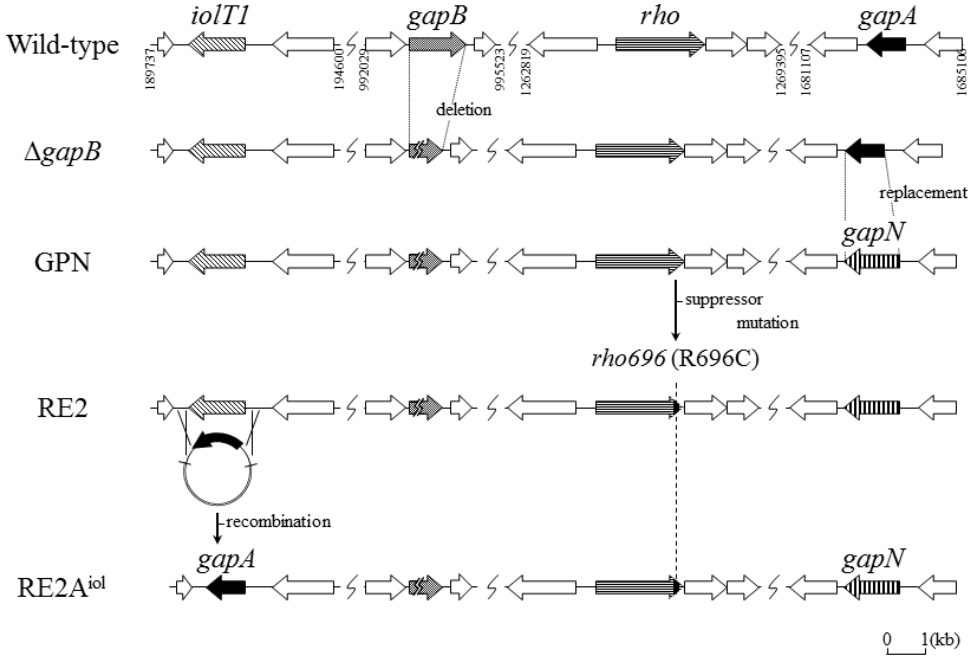

Fig. 3. Takeno

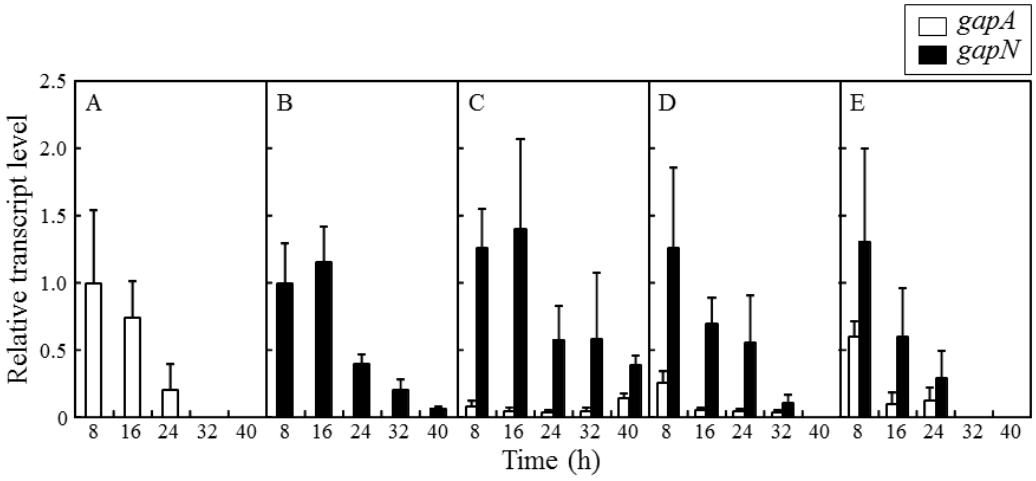
gapA
gapN
A
B
C
D
E
Relative transcript level
2.5
2.0
1.5
1.0
0.5
0
8 16 24 32 40 8 16 24 32 40 8 16 24 32 40 8 16 24 32 40 8 16 24 32 40
Time (h)

Fig. 4. Takeno

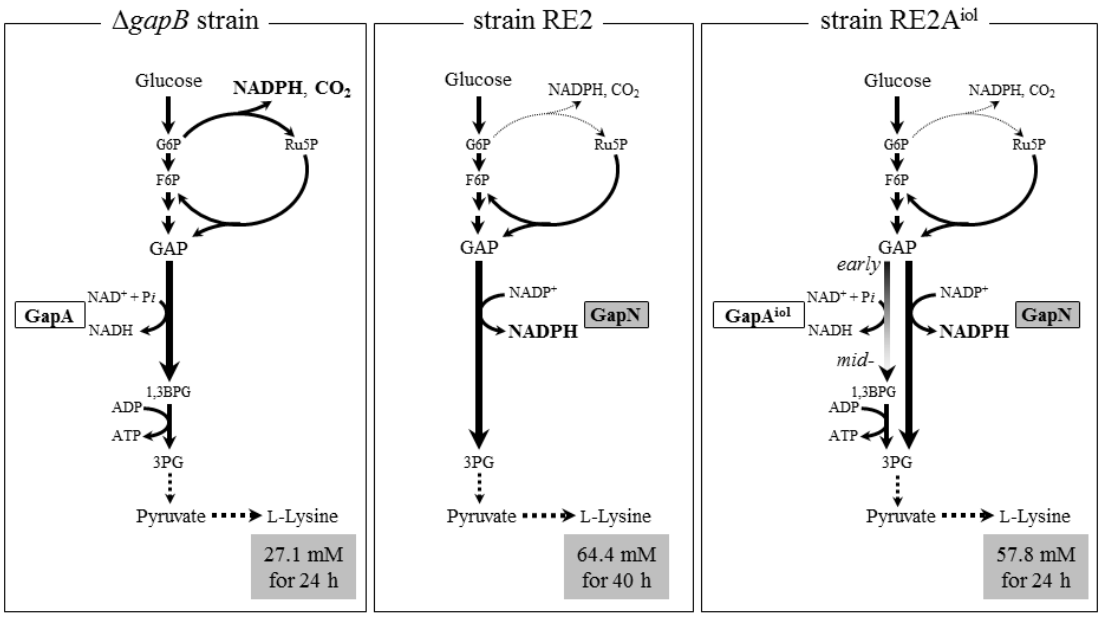
Δ*gapB* strain
Glucose
NADPH, CO2
G6P
Ru5P
F6P
GAP
GapA
NAD+ + Pi
NADH
1,3BPG
ADP
ATP
3PG
Pyruvate
L-Lysine
27.1 mM
for 24 h
strain RE2
Glucose
NADPH, CO2
G6P
Ru5P
F6P
GAP
NADP+
NADPH
GapN
3PG
Pyruvate
L-Lysine
64.4 mM
for 40 h
strain RE2A^iol
Glucose
NADPH, CO2
G6P
Ru5P
F6P
GAP
early
GapA^iol
NAD+ + Pi
NADH
NADP+
NADPH
GapN
mid-
1,3BPG
ADP
ATP
3PG
Pyruvate
L-Lysine
57.8 mM
for 24 h

Fig. 5. Takeno